Research Article Vol. 55, No. 26 / September 10 2016 / Applied Optics 7265

applied optics

Traceability of solar UV measurements using the QASUME reference spectroradiometer

GREGOR HÜLSEN,[1,*] JULIAN GRÖBNER,[1] SAULIUS NEVAS,[2] PETER SPERFELD,[2] LUCA EGLI,[1] GEILAND PORROVECCHIO,[3] AND MAREK SMID[3]

[1]Physikalisch-Meteorologisches Observatorium Davos, World Radiation Center (PMOD/WRC), Davos, Switzerland
[2]Physikalisch-Technische Bundesanstalt (PTB), Bundesallee 100, 38116 Braunschweig, Germany
[3]Cesky Metrologicky Institut (CMI), Brno, Czech Republic
*Corresponding author: gregor.huelsen@pmodwrc.ch

Received 10 June 2016; revised 10 August 2016; accepted 11 August 2016; posted 12 August 2016 (Doc. ID 268096); published 7 September 2016

One major objective of the European Joint Research Project "Traceability for surface spectral solar ultraviolet (UV) radiation" was to reduce the uncertainty of spectral UV measurements. The measurement instrument used for this work was the portable UV European reference spectroradiometer QASUME. The calibration uncertainty of this instrument was decreased and validated by a comparison of direct calibrations against a primary standard for spectral irradiance, a high temperature blackbody radiator, and against a reference detector using a spectrally tunable laser as a monochromatic source. The spectral irradiance responsivity of the reference detector is traceable to the primary standard of optical power, realized through a cryogenic radiometer, and to the SI unit of meter. The measuring technique was improved by the construction of a new reference spectroradiometer, QASUMEII. An improved input optics removes the dependences of the measured solar irradiance on the angle of incident for solar zenith angle smaller than 75 deg. Moreover, a hybrid photon detection system enables continuous tracking of the instrument's responsivity changes. For both spectroradiometer systems an uncertainty budget was calculated. The improvements have reduced the measurement uncertainties of solar spectral UV irradiance measurements from 4.8% in 2005 to 2.0% ($k = 2$) in the spectral region above 310 nm. The largest sources of uncertainty were the absolute spectral irradiance responsivity calibration, the angular response uncertainty, and the instrument stability using the hybrid detector, which were reduced from 3.6% to 1.1%, from 1.2% to 0.6%, and from 0.65% to 0.4%, with respect to the situation prior to the project. The new instrument was validated during a four month intercomparison relative to the QASUME reference. The mean ratio of the solar irradiance scans between the two reference spectroradiometers has an offset of $+0.7\%$ and a standard deviation of $\pm 1.5\%$ for a wavelength greater than 305 nm, which is well within the combined uncertainty of 3.7% calculated from the uncertainties of the two systems.

OCIS codes: (010.1290) Atmospheric optics; (120.0120) Instrumentation, measurement, and metrology; (120.3940) Metrology; (120.5630) Radiometry; (120.6200) Spectrometers and spectroscopic instrumentation; (260.7190) Ultraviolet.

http://dx.doi.org/10.1364/AO.55.007265

1. INTRODUCTION

The observation and understanding of long-term changes in terrestrial solar ultraviolet (UV) radiation over the next decades is important for human health protection. In order to quantify and monitor long-term changes of global UV radiation at the Earth's surface, accurate measurement techniques are required. Long-term trends in surface solar radiation due to atmospheric-induced changes have demonstrated decadal changes of the order of 2% per decade over Europe [1] in the time period from 1960 until 2000. These changes are currently explained by changes in the transparency of the atmosphere and possibly long-term changes in clouds. The effects of these changes on UV radiation have not yet been quantified due to the difficulty of observing these small changes over such long time scales. Future changes in the UV radiation due to atmospheric changes are expected to be of the same order of magnitude and require measurements with significantly lower uncertainties as stated in [2] of around 1%–2% to detect such decadal changes.

Solar UV radiation observations with high-quality instruments are limited to a few places worldwide. To assess the quality of these stations the portable reference spectroradiometer known as "QASUME" performed more than 65 site visits at 33 European stations since 2001 [3].

To address the above-mentioned challenges, the Joint Research Project "Traceability for surface spectral solar ultraviolet radiation" (SolarUV) was carried out from 2011 to 2014 within the European Metrology Research Programme (EMRP), jointly funded by the EMRP participating countries within the European Association of National Metrology Institutes (EURAMET) and the European Union. Its main aim was to significantly enhance the reliability of spectral solar UV radiation measurements in the wavelength range from 280 to 400 nm by the development of new methods of observation and by providing traceable solar UV irradiance measurements with uncertainties of 2% or less. The project shortened the traceability chain of the solar UV measurements to the SI unit and reduced the associated transfer uncertainties by the use of state-of-the-art technologies, such as a tunable laser facility from a National Metrology Institute (NMI).

As part of the project, a second portable reference spectroradiometer, called QASUMEII, was constructed, fitted with an improved global entrance optic and a newly developed hybrid device, consisting of a photomultiplier and a solid-state detector. This paper presents the validation of the new spectroradiometer against QASUME in 2015 and, as a final outcome of the project, an updated uncertainty budget for spectral solar UV irradiance measurements, based on a comprehensive assessment of the instrument characteristics.

2. TRACEABILITY CHAIN OF GLOBAL SPECTRAL UV IRRADIANCE MEASUREMENTS

The absolute spectral responsivity of a spectroradiometer is usually determined by measuring the radiation from calibrated transfer standards (TS). These TS devices are typically 1000 W tungsten halogen lamps. The irradiance output of the TS—at a specific orientation, distance, and electric current value—is calibrated against secondary standards, which usually are halogen lamps of the same type. The secondary standard lamps themselves are calibrated against primary standards for spectral irradiance, such as high temperature blackbody cavities at NMIs. The aperture size of the blackbody as well as the distance to the reference plane for measurements and the blackbody temperature itself are important parameters for the spectral irradiance realization. Broadband filter radiometers are used to determine the blackbody temperature. Their spectral responsivity is calibrated against a silicon trap detector, which is directly calibrated against an absolute cryogenic radiometer. Through this source-based traceability chain (Fig. 1, right side) the TS irradiance calibration is linked to the SI units in $\mathrm{W m^{-2}\,nm^{-1}}$ where each step of this chain adds uncertainties to the final measurement.

The transportable reference spectroradiometer system QASUME was validated for the first time in 2004 by a direct calibration against the primary standard of spectral irradiance, the blackbody BB3200pg from the Physikalisch Technische Bundesanstalt (PTB), Braunschweig, Germany [4]. This procedure shortens the traceability chain as demonstrated in Fig. 1 (dashed arrow). During the SolarUV project this validation was repeated two times in 2013 and 2014, respectively, using the 1000 W transfer standards as well as a QASUME responsivity monitoring scheme based on low-power 250 W tungsten

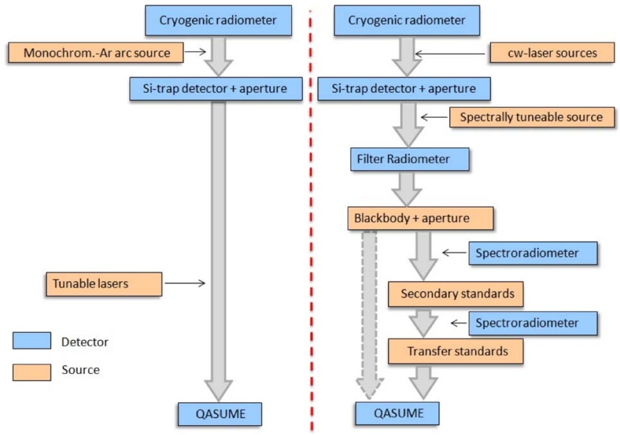

Fig. 1. Traceability chains for the calibration of the reference spectroradiometer QASUME: it can be realized by means of calibration sources, as shown to the right from the vertical line, or by using a calibrated detector and wavelength-tunable lasers, as shown on the left part of the figure.

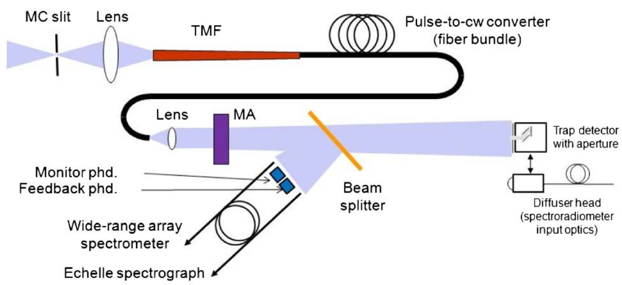

Fig. 2. Schematic representation of a beam conditioning unit in the TULIP facility used to convert the beam of a mode-locked fs-pulsed tunable laser into a uniform, stable, and depolarized radiant field necessary for the irradiance-mode calibrations. MA, microlens array; TMF, tapered multimode fiber; MC, monochromator.

halogen lamps in a custom-made portable calibrator housing. The QASUME spectral irradiance responsivity is calibrated annually in the optical laboratory of the World Calibration Center for UV (WCCUV), against a group of seven spectral irradiance standard lamps directly calibrated by the PTB, and the calibration results are transferred to the low-power monitor lamps by taking the respective spectroradiometer readings.

The calibration of the spectral responsivity of the QASUME spectroradiometer can also be realized by comparison with a reference detector by the help of wavelength-tunable lasers facilities (Fig. 1, left side). As shown in Fig. 1, this traceability route to the primary standard of optical power, a cryogenic radiometer, is shorter, and, thus, a reduction of the associated transfer uncertainties could be expected. In order to enable this calibration scheme, however, a uniform and quasi-monochromatic radiant field with a sufficiently high irradiance level needs to be generated. The realization of this calibration approach was accomplished within the SolarUV project. For that purpose, the wavelength-tunable laser facility at the PTB, Tunable

Lasers in Photometry (TULIP) [5], was upgraded by a mode-locked femtosecond (fs)-pulsed laser and prepared for the operations throughout the solar UV spectral range from 280 to 400 nm and beyond. To enable the irradiance-mode calibrations at the TULIP facility in this spectral range, a laser monochromator has been set up allowing an efficient bandpass reduction below 0.1 nm full width half-maximum (FWHM) and an active stabilization for the laser power has been implemented enabling a short-term fluctuation of the flux to be controlled at the level of 10^{-4}. Additionally, a beam conditioning unit providing a spatially homogeneous and depolarized field qualified for calibrations in the irradiance mode has been developed. Figure 2 depicts schematically the beam conditioning setup in the laboratory. The traceability to the primary standard for radiant power, a cryogenic radiometer of the PTB, is provided by silicon trap detectors built and characterized for this purpose. The transfer to irradiance responsivity has been realized using a radiometric aperture with a calibrated area.

For a narrowband laser radiation of a chosen laser wavelength λ_0, the irradiance $E(\lambda_0)$ of the generated uniform field at the measurement position can be measured by a calibrated trap detector with spectral power responsivity $s_{\mathrm{Trap}}(\lambda_0)$ and a calibrated aperture of area A set in front of the detector:

$$E(\lambda_0) = \frac{Y_{\mathrm{Trap}}(\lambda_0)}{s_{\mathrm{Trap}(\lambda_0)}} \cdot A \cdot \prod_{j=1}^{6} b_j(\lambda_0), \tag{1}$$

where $Y_{\mathrm{Trap}}(\lambda_0)$ denotes the photocurrent measured by the trap detector and $b_j(\lambda_0)$ denotes adjustment factors allowing to correct for nonideal properties of the detectors and the measurement conditions: nonuniformity of the detector active area and that of the field, spatial stray light, nonlinearity, distance settings, laser wavelength, and stability of the field. The signal of the QASUME spectroradiometer $Y_Q(\lambda_0)$ at the same wavelength λ_0 integrated throughout its bandpass can be expressed as

$$Y_Q(\lambda_0) = \prod_{j=1}^{6} a_j(\lambda_0) \cdot \int s_Q(\lambda_0, \lambda) \cdot E_\lambda(\lambda) \mathrm{d}\lambda, \tag{2}$$

where $E_\lambda(\lambda)$ is the spectral irradiance of the laser field (see Fig. 3), $s_Q(\lambda_0, \lambda)$ is the spectral bandpass function of the spectroradiometer at a wavelength λ_0 and $a_j(\lambda_0)$ are adjustment factors for the QASUME measurements: determination of diffuser reference plane, spatial nonuniformity, spatial stray light, accuracy of monochromator scan, photomultiplier tube (PMT) nonlinearity, and stability of the instrument. The adjustment factors a_j and b_j in measurement Eqs. (1) and (2) were set to a value of 1. However, every factor has an associated uncertainty. The meaning of individual adjustment factors and the respective uncertainties for measurements at the TULIP setup are discussed in detail in [6].

The QASUME signal $Y_Q(\lambda_0, \lambda)$ at a laser wavelength setting λ_0 can be measured by scanning its wavelength λ from, e.g., $\lambda_0 - 2 \cdot \mathrm{FWHM}$ to $\lambda_0 + 2 \cdot \mathrm{FWHM}$, where FWHM is the full width at half-maximum of the instrument's bandpass function. So that the responsivity of the spectroradiometer at the wavelength λ_0 can be expressed as the quotient of the spectrally integrated spectroradiometer signal Eq. (2) and the irradiance measured by the trap detector Eq. (1):

$$s_Q(\lambda_0) = \frac{Y_Q(\lambda_0)}{E(\lambda_0)}. \tag{3}$$

Two measurement campaigns involving both the calibration of the QASUME spectroradiometer at the TULIP facility against the trap detectors and a direct measurement of spectral irradiance by the high-temperature blackbody were arranged in the spring of 2013 and of 2014.

Figure 4 summarizes the results of all the calibrations of the QASUME carried out at the PTB. The figure shows ratios of irradiances as measured by the QASUME and PTB values. Solid curves show such ratios for the direct blackbody

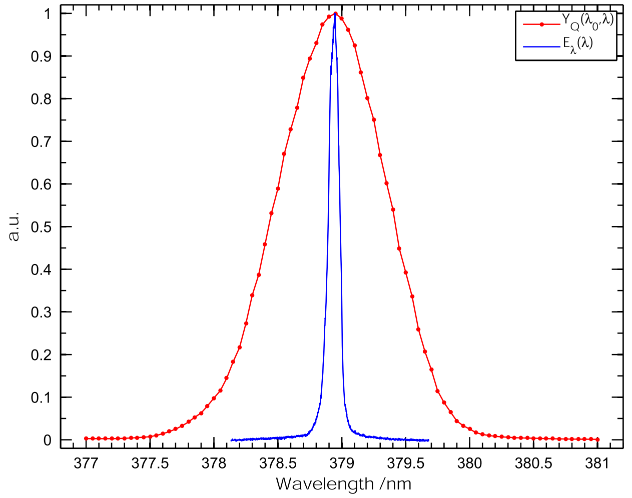

Fig. 3. Example of a wavelength-dependent QASUME signal $Y_Q(\lambda_0, \lambda)$ measuring a narrowband laser irradiance $E_\lambda(\lambda) \cong E(\lambda_0)$. The spectral width of the QASUME signal recorded by wavelength scanning is defined by its bandpass function.

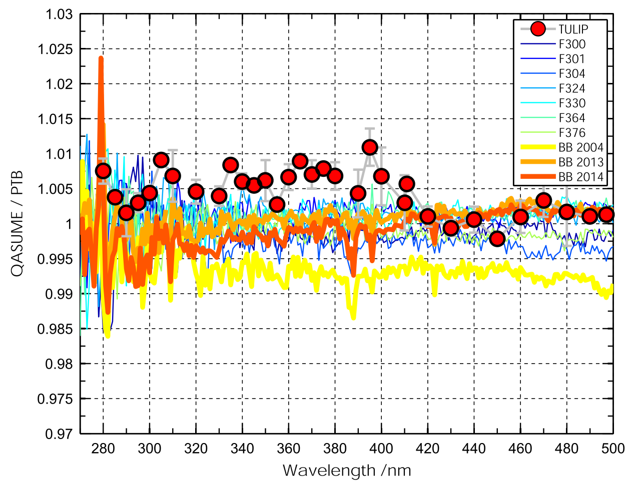

Fig. 4. Agreement among irradiances measured by the QASUME and the respective PTB values. Compared were measurements on the WRC/WCCUV irradiance standard set (F300 till F376), the BB3200pg blackbody in 2004, 2013, and 2014 at PTB, and the laser generated irradiances at the tunable laser setup TULIP at PTB.

measurements carried out in 2004, 2013, and 2014, as well as for the lamp transfer standards F300 to F376 representing the irradiance scale of QASUME. The filled circles show such ratios for the irradiances of the laser field at the TULIP facility when measured by the QASUME and the reference detector. The results demonstrate the excellent reproducibility and stability of the QASUME irradiance calibrations traced to the blackbody via a source-based traceability chain. An agreement between the two totally different calibration approaches as shown in Fig. 1 was proven to be within 1% below 400 nm.

3. IMPROVED PORTABLE REFERENCE SPECTRORADIOMETER QASUMEII

The main design features of the new transportable reference spectroradiometer QASUMEII are based on the existing QASUME system [2]. The core part of the instrument is a Bentham DM150 double monochromator with a focal length of 150 mm and two 2400 lines/mm gratings arranged in subtractive dispersion mode. The radiation is collected by a Bentham D6 input optic and guided by a quartz fiber bundle to the entrance slit of the monochromator. A new hybrid detection system is used to measure the output signal (see Section 3.B). The slit width of the monochromator is fixed to 0.56 mm, which results in a nearly triangular slit function of 0.86 nm FWHM. To ensure outdoor measurements, the Bentham DM150 is mounted inside a temperature-controlled transportable weather-proofed box.

A. Input Optic

The angular response of the Bentham D6 entrance optic was measured at the WCCUV laboratory at Physikalisch-Meteorologisches Observatorium Davos, World Radiation Center (PMOD/WRC). Figure 5 shows that the deviations with respect to the nominal angular response error are less than 2% for zenith angles smaller than 75 deg. The integrated cosine error is 1.005 ± 0.003 at 350 nm.

Because of the temperature sensitivity of the Teflon (PTFE) diffuser, an environmental control case was built for the D6 optic (Fig. 6). Using a silica gel cartridge the relative humidity is kept below 10% and the temperature is kept above 30°C by in-built heating, well above the phase transition of PTFE at 19°C [7].

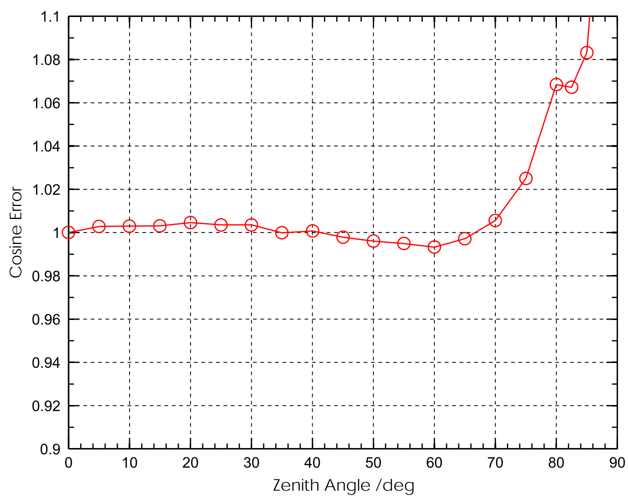

Fig. 5. Cosine error of the Bentham D6 cosine diffuser at 350 nm.

Fig. 6. Environmental control case for the input optics.

B. Photon Detection System

A new solid-state detection system (SSDS) has been developed [8] with the aim of improving the overall performance of PMTs commonly used in double monochromator spectroradiometer systems employed for the detection of solar UV radiation. Although the PMTs are the detectors of choice for measuring solar UV radiation due to their high sensitivity, the disadvantage is the instability, such as hysteresis effects due to high illumination, causing sensitivity variations of 2% or more.

The SSDS is composed of the latest generation UV-optimized photocounter from Hamamatsu H11890 in conjunction with state-of-the-art silicon photodiodes with custom-made high-sensitivity electronics based on the switched integrator principle (SIA) [9]. Both detectors, the photocounter and three Si diodes connected in parallel, are placed at the exit slit of the double monochromator, so that they can sample the output radiation simultaneously.

The photocounter is a small form factor device with a sensitive area of 50 mm^2 controlled via USB. The device's sensitivity is similar to that of a PMT but it has the advantage of a much smaller size. It has a peak responsivity of $5 \cdot 10^5$ counts/s/pW at 400 nm that drops to $3 \cdot 10^5$ counts/s/pW at 280 nm, which is sufficient to detect even the lowest range of the solar UV spectrum. Its dark count is below 40 counts/s and the device is linear up to $2 \cdot 10^6$ counts/s. Figure 7 shows the front side of the SSDS hybrid detector. The position of the SSDS along the vertical axis relative to the exit slit of the monochromator was adjusted manually to optimize the radiation sampled by the Si diodes and the photocounter, respectively.

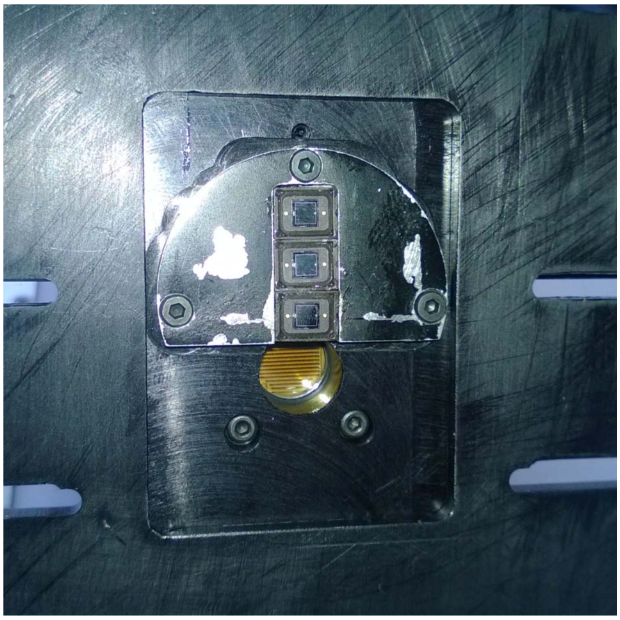

Fig. 7. Front side of SSDS showing the three silicon photodiodes connected in parallel, lined up above the entrance window of the photocounter.

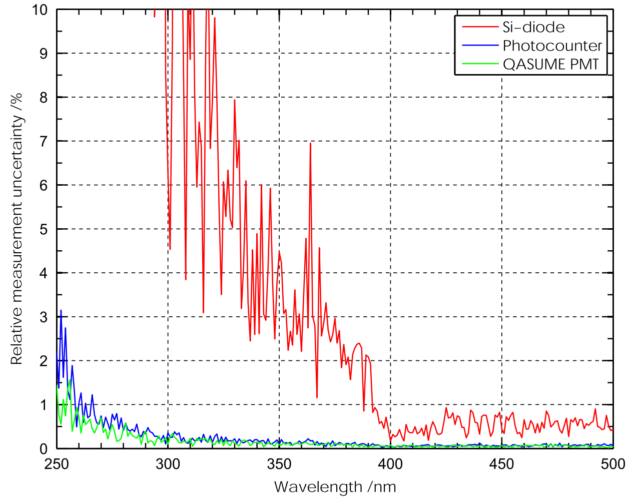

Fig. 8. Relative measurement uncertainty as function of the wavelength of a 250 W portable monitoring lamp calibration as function of the wavelength using the Si diode (red line), the photocounter (blue line), and the QASUME PMT (green line).

The readout electronics for the silicon diodes—a microcontroller-driven switched integrator principle design—has been developed by the Czech Metrology Institute, Brno, Czech Republic. The electronics offers up to 7 orders of magnitude of dynamic range and the integration time is generated on the printed circuit board. In order to further extend the sensitivity of the SIA-based detection system to lower power levels a small area/low dark current silicon detector has been selected (Hamamatsu 1227 33BQ). The timing constraint of 1 s for each measurement point given by the QASUME standard measurement procedure led to the selection of a 1 pF integration capacitor with PTFE as dielectric material that offers the lowest leakage current, a critical parameter for the switched integrator amplifier in this context. Particular care has been taken to minimize any source of leakage current in the circuit: all the critical electric paths are in air. Furthermore, to reduce noise pickup the connections between the photodiode and amplifier have been made as short as possible and the whole system is enclosed in a grounded aluminum shield. The latest prototype has shown excellent noise performance of 3 $\mathrm{fW/Hz^{\frac{1}{2}}}$ and stability better than 5 fA of dark signal in 10 h. The stability of the dark signal makes it possible to measure its value only at the beginning of the solar spectrum measurement.

The SSDS offers the high sensitivity of the photocounter necessary to detect the portion of the solar UV spectrum with low irradiance levels (in particular in the UVB part) in conjunction with the stable and linear behavior of the Si diode [10] to cover the region with higher irradiance level.

The performance of the SSDS was initially tested in the laboratory using artificial 250 W radiation sources. The relative measurement uncertainty of the signal recording with the two detectors is shown in Fig. 8. Both calibrations were performed using a 0.1 s integration time with 10 samples per wavelength increment. The Si diode responsivity calibrations can be used for wavelengths above 400 nm but not for the UV wavelength range between 280 and 400 nm, while the relative measurement uncertainty of the photocounter part of the SSDS is below 0.5% for wavelengths greater than 280 nm.

Figure 9 illustrates the performance of the SSDS for outdoor sun radiation measurements on a clear-sky summer day (18th July 2015) using standard QASUME measurement parameters (integration time of 0.1 s, seven samples per wavelength increment). The relative measurement uncertainty is below 0.2% for the Si diode data for wavelengths between 420 and 460 nm throughout the whole day. The performance of the photocounter is significant better. The S/N exceeds 0.2% only at very

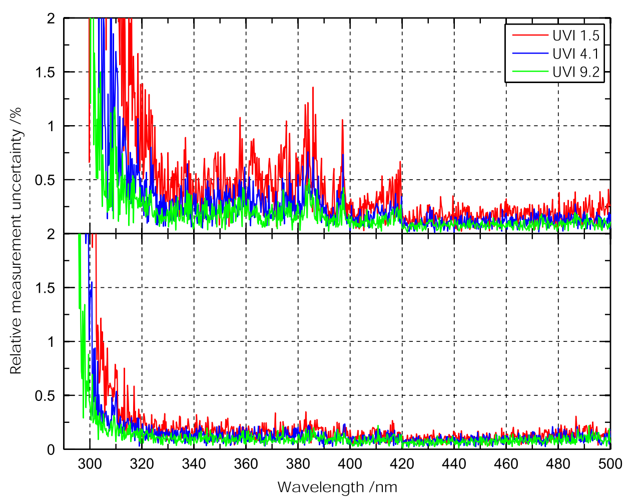

Fig. 9. Relative measurement uncertainty of solar UV recordings as function of the wavelength for the Si diode (top) and the photocounter (bottom) for different irradiance levels in the early morning (red, UVI 1.5), morning (blue, UVI 4.1), and at noon (green, UVI 9.2).

low wavelengths: for high irradiance levels with a UV index (UVI) above 9 this cutoff wavelength is 305 nm, for a UVI around 4 it is 315 nm and for a UVI below 2 it is 325 nm, which is comparable to the performance of QASUME.

C. Linearity

The exposure of the detector with photons is a random process exhibiting a Poisson distribution [11]. Photon-counting detectors have a small dead time after the arrival of a photon. Depending on the photon arrival rate a well-defined number of photons arrive faster than the resolving time of the detector electronics and are thus not counted, which is known as the dead-time effect. Knowing the so-called pulse pair resolution, the nonlinearity of the output signal can be corrected using a dead-time correction. For the correction of the QASUMEII data the following equation is used:

$$N = \frac{M}{1 - M \cdot dT}, \tag{4}$$

with the real count rate, N, and the measured count rate, M, in s^{-1} and the pulse pair resolution, dT, in seconds [11]. The H11890 photon counter has a nominal dead time of 20 ns (Hamamatsu H11890 Datasheet), which was confirmed in tests performed in the optical laboratory at PMOD/WRC, as shown in Fig. 10. In the experiment the count rate of the photocounter was measured using a 1000 W FEL lamp at high and low radiation levels. Figure 10 shows in red the normalized ratio of the two measurements taking the raw counts of the photocounter signal and in blue using the dead-time-corrected count rate, respectively. As seen in Fig. 10 the dead-time-corrected counts are independent of the count rate.

This detector property limits the dynamic range of the detector. To limit the correction factors to below 10%, neutral density filters (ND) are used to reduce the incident radiation on the detector. Figure 11 shows the attenuation of the selected filters. At 350 nm the attenuation of the ND 1.0 filter is

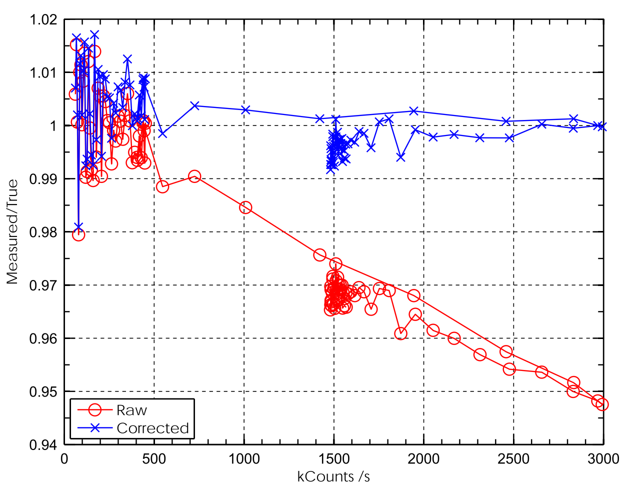

Fig. 10. Nonlinearity measurement of the Hamamatsu photon counter. The red line corresponds to the raw data of the detector and in blue the corrected data using Eq. (4) with a dead time of 20 ns is shown.

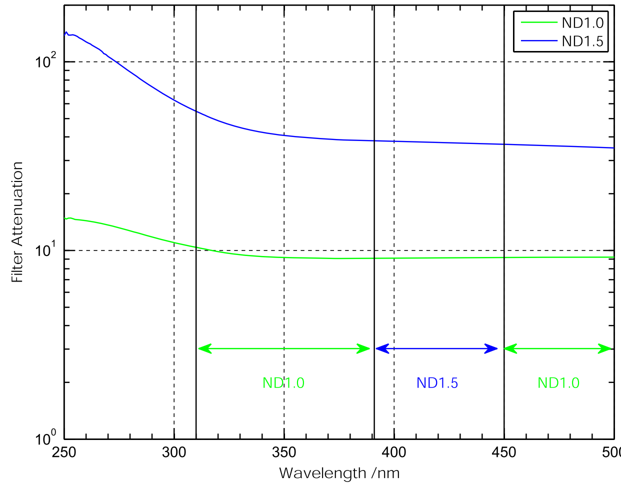

Fig. 11. Attenuation of the selected neutral density filters. The wavelength ranges where they are used are indicated by the green (ND 1.0) and blue (ND 1.5) arrows.

9.197 ± 0.045 and at 420 nm it is 37.378 ± 0.187 for the ND 1.5 filter.

D. Operating Mode of QASUMEII

Spectral global solar UV measurements using QASUME are carried out in the wavelength range from 290 to 400 nm or up to 500 nm, with increments of 0.25 nm. The use of an integration time of 0.7 s and a spare time of 0.8 s leads, thus, to 11 min or 21 min per scan of one solar irradiance spectrum, respectively. Using these parameters the Si diode of the SSDS cannot measure the signal with sufficient relative measurement uncertainty for wavelengths below 420 nm (see Fig. 9). Therefore, the photocounter is used as the primary detecting device.

The advantage of the solid-state detector is the long-term stability. The Si diode is therefore used to monitor the overall stability of the QASUMEII system. This is done by parallel measurements of the solar signal with both detectors before and after a solar irradiance scan. As relative responsivity changes were found out to be spectrally neutral, monitoring at a single wavelength, i.e., at 450 nm, is sufficient to track the changes at the overlapping region between 420 and 500 nm only and to apply the single correction factor for the entire spectrum. This responsivity monitoring and correction technique will be referred to here as SSDSratio. Technical details are presented in Section 4.

4. VALIDATION OF QASUMEII USING QASUME

The new reference spectroradiometer QASUMEII was validated against QASUME during a 4-month measurement campaign in 2015. The standard protocol for global UV spectroradiometer intercomparison was used for the validation, which is defined as follows: synchronized scans were acquired from sunrise to sunset every half an hour for the wavelength range 290–500 nm with 0.25 nm increments. The systems were calibrated around one to three times per month using 250 W lamps in a portable calibrator.

For clear-sky days the data of QASUME were corrected for the cosine error of the input optic. This correction is a function of the solar zenith angle (SZA) and reaches values of up to +2%. For QASUMEII the cosine correction is negligible because of the low cosine error (Fig. 5), thus, no correction was applied. For diffuse-sky conditions the diffuse cosine correction function is close to unity for both instruments and no correction is necessary. Data recorded during mixed-sky conditions were left uncorrected.

The temperature of both input optics was recorded to check the stability of the housing and to apply a temperature correction to account for transmission changes of the Teflon. Both datasets were further processed using the matSHIC algorithm [12], which performs a deconvolution technique based on a high-resolution reference solar spectrum to adjust the wavelengths and the spectral resolution of the measured solar spectrum to this reference spectrum by a correction [13]. Finally, a homogenized solar spectrum with a nominal resolution of 1 nm is obtained.

The validation campaign in 2015 started on day of year (DOY) 196, 15th July, and lasted until DOY 300, 27th October. Five interrupts occurred for the following DOYs:

- 205–207: Maintenance of QASUME.
- 213–214, 226–231: Malfunctioning of QASUME (filter movement problems).
- 240–271: QASUME was used for a site audit in Austria and for lamp calibrations.
- 295–298: Maintenance of QASUMEII.

During the period of DOY 217 until 236 both spectroradiometers recorded the solar irradiance only up to 400 nm because these reference datasets were used for broadband radiometer calibrations.

The calibration of both QASUME systems was checked and corrected for drift regularly during the course of the comparison using the portable 250 W lamps. The change in responsivities of both systems is shown in Fig. 12: QASUME (top) stayed within ±1%, whereas the responsivity of QASUMEII (bottom) changed by 3% after DOY 245 due to a repair of the entrance optics, including a readjustment of the fiber bundle, and a consequent change in the illumination of the entrance slit of the monochromator. The responsivity remained constant to within ±1% after that intervention. On DOY 265 new ND filters were fitted into the filter wheel of QASUMEII. This modification caused the change in the responsivity of around 2%. The humps in the wavelength region where the transmission of QASUME and QASUMEII changes rapidly (between 380 and 400 nm, see Fig. 13)—seen especially on DOY 239 (magenta curve, top) and DOYs 194 and 218 (blue and red curves, bottom)—indicate a possible small wavelength shift of the spectroradiometer. However, for solar UV measurement data these wavelength shifts are corrected using the matSHIC algorithm.

The long-term stability of the Si diode, important for the SSDSratio measurement, was validated against the 250 W lamp calibrations. Figure 14 shows a good agreement between these two monitoring schemes. The data of the QASUMEII

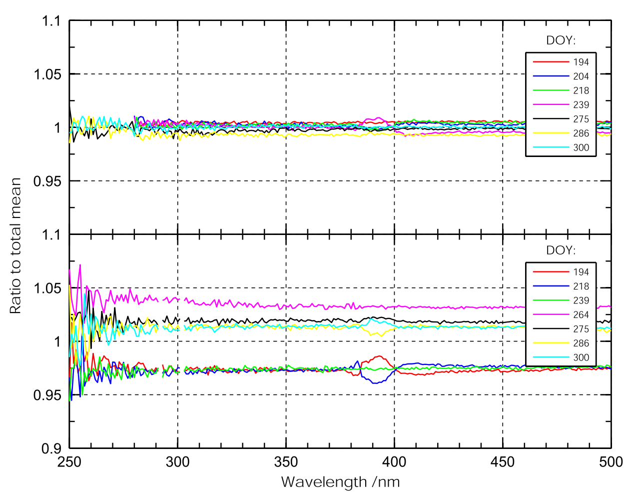

Fig. 12. QASUME (top) and QASUMEII (bottom) responsivity change during the spectroradiometer intercomparison in 2015.

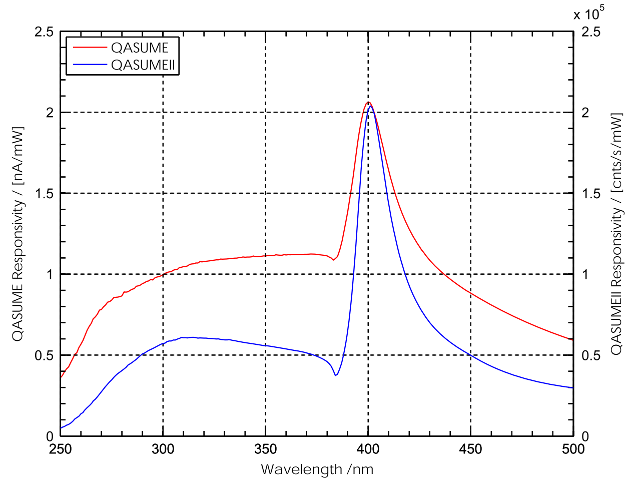

Fig. 13. Spectral responsivities of QASUME (red) and QASUMEII (blue) measured using 250 W lamps on DOY 300, 2015.

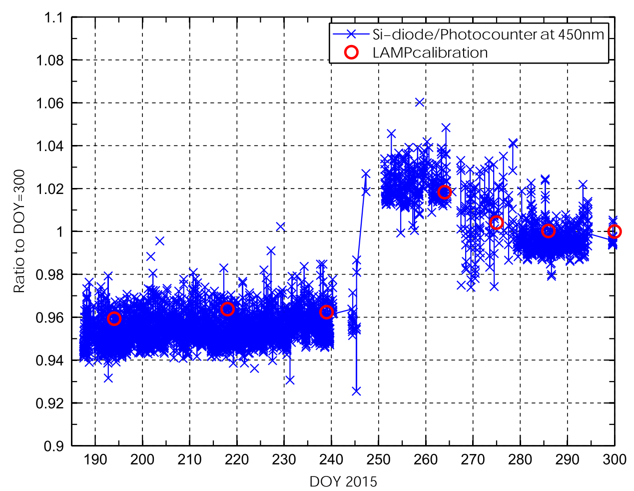

Fig. 14. QASUMEII responsivity change as detected by Si diode to photocounter ratio at 450 nm (blue) and the lamp calibrations of the system using the photocounter detector (red circles).

photocounter spectral responsivity calibrations (Fig. 12, bottom) using the 250 W monitor lamps were averaged for the comparison in the wavelength band 450 nm ± 2.5 nm.

The SSDSratio measurement does not only reveal long-term responsivity changes of the system but also a diurnal variably. During a clear-sky day the responsivity of the photocounter changed up to 3% because of the large increase of the UV irradiance while the Si diode responsivity remained constant. The respective UV index during the day changed from 0 to 8.5. The resulting diurnal change of the SSDSratio (see Fig. 15, top) is used to compensate for this observed variability. A second-order polynomial correction function is fitted to the data points with SZA $< 75^{\circ}$. If the relative uncertainty of the selected data points is above 1% and fewer than seven points have been selected a mean offset is calculated as correction value. During diffuse or cloudy days the signal increase throughout the day is much smaller and, thus, the variability of the SSDSratio is less than ±0.5% (Fig. 15, bottom).

Summarized results of the validation campaign are shown in Figs. 16 and 17. The first figure shows the spectral average ratio of QASUMEII to QASUME data obtained from 1443 out of 2060 synchronized solar irradiance scans. Rain, fast moving clouds, and manual disturbances during a synchronized scan do not permit a comparison of the two datasets. Thus, scans recorded under such conditions were manually removed from the analysis. The mean ratio of the 1443 scans has an offset of +0.7% and a standard deviation of ±1.5% for wavelengths longer than 305 nm.

The performance of the QASUME systems throughout the intercomparison period in individual wavelength bands is shown in Fig. 17, which displays the mean spectral ratio between QASUMEII to QASUME for the wavelength bands at 310, 350, and 495 nm. The bands have a width of ±2.5 nm. The five thick vertical lines indicate the interrupts mentioned above. Only a few outliers of the comparison points are not within the uncertainty of the comparison, $U = \pm 3.7\%$ ($k = 2$, see Section 5):

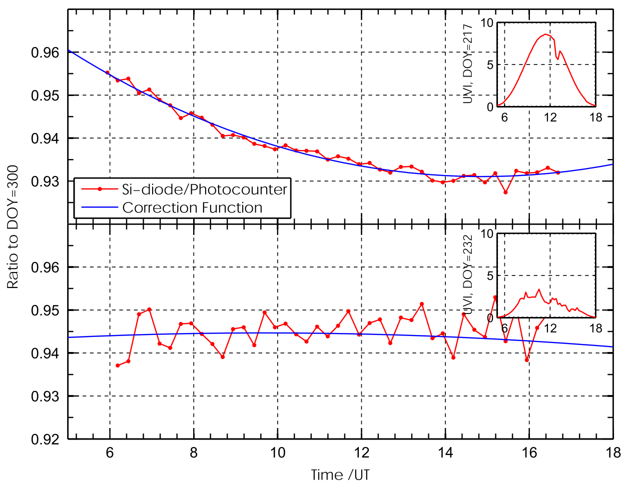

Fig. 15. Diurnal variability of the Si diode to the photocounter signal ratio during a clear-sky day (top) with a large irradiance change (see insert) and during a diffuse-sky day (bottom) with a lower UVI. The blue lines indicate the fitted correction function used to compensate for the photocounter hysteresis.

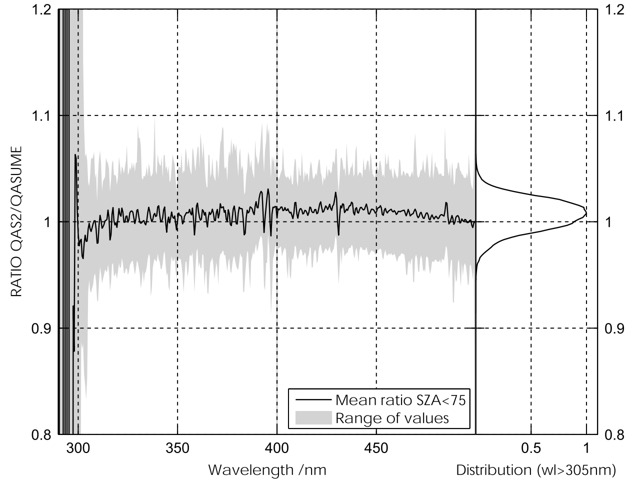

Fig. 16. Mean ratio of 1443 synchronized solar irradiance scans between the two reference spectroradiometers for the whole intercomparison period has an offset of +0.7% and a standard deviation of ±1.5% for wavelengths longer than 305 nm.

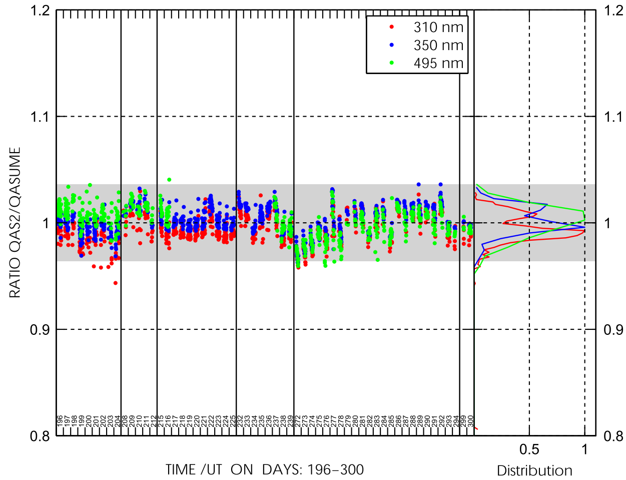

Fig. 17. Mean ratios between the two reference spectroradiometers at selected wavelength bands are within the uncertainty of the comparison (gray shadowed area).

$$U = \sqrt{U_{\text{qas}}^2 + U_{\text{qas II}}^2}. \tag{5}$$

Within this uncertainty a minor systematic variability can be seen. Most of the features can be explained:

- After the third interruption (five-day-long filter malfunctioning of QASUME) the responsivity of QASUME changed, which caused the increase of the ratio on DOY 232 by 2%. The recalibration of QASUME on DOY 239 was performed too late to detect this temporal responsivity change.
- The lower ratio on DOY 272, which increases to unity until DOY 275, can be attributed to the warm-up phase of QASUME after the return from the site audit in Austria. The calibration of this instrument was performed on DOY 275.

• Larger daily variabilities, like, e.g., on DOY 277, are due to the fact that the cosine correction of QASUME is only possible during well-defined clear-sky measurement conditions. The mentioned example, however, includes overcast conditions in the morning and clear sky in the afternoon. This illustrates the limitation of a cosine correction and the need for high-quality entrance optics with reduced cosine error.

• Additional small variabilities are introduced by temperature changes of the input optic, which are not fully compensated by both the temperature control of the devices and the correction function for these changes.

These variabilities add up to the overall uncertainty of the measurements discussed in the following section.

5. UNCERTAINTY OF SPECTRAL GLOBAL SOLAR UV MEASUREMENTS

The uncertainty budget for solar UV measurements using QASUME and QASUMEII is summarized in Table 1. The estimation of the various uncertainty components is based on the procedure outlined in [2], with reduced uncertainty values due to the improved characterizations and calibrations developed during the SolarUV project. The uncertainty contributions shown in Table 1 are described below.

A. Radiometric Calibration

The radiometric traceability chain was described in Section 2. The spectral irradiance scale of the QASUME is established using seven 1000 W tungsten halogen transfer standards calibrated directly against the primary spectral irradiance standard of the PTB. At PMOD/WRC, the irradiance scale is transferred annually to a set of 250 W portable monitoring lamps used to calibrate QASUME or QASUMEII when they are deployed outdoors for solar UV measurements. A description of the portable calibration system is described in [2] and has not changed since then.

The reduction of uncertainty in the radiometric calibration is primarily due to an improvement at the top of the traceability chain, e.g., the uncertainties of the transfer standards calibrated at the PTB, from a standard measurement uncertainty of 1.5% between 300 and 400 nm [4] to ~0.4%. This reduction could be achieved by calibrating the transfer standard lamps directly against the blackbody as the primary standard of the PTB.

Furthermore, by using a set of seven transfer standards each calibrated directly against the blackbody of the PTB, and taking into account the correlation of these transfer standards between each other [14], the standard radiometric uncertainty of QASUME finally results to 0.55%. The QASUME calibration against a reference detector using the spectrally tunable laser source as described in Section 2, can be carried out also with an estimated uncertainty of 0.54% [15].

Table 1. Uncertainty Budget for Solar UV Measurements Using QASUME and QASUMEII[a]

Uncertainty Parameter	Relative Std Uncertainty/% QASUME	Relative Std Uncertainty/% QASUMEII
Radiometric calibration$_{\lambda \geq 300\,\mathrm{nm}}$	0.55	
250 W lamp stability$_{\text{one year}}$	0.14	
Nonlinearity$_{\text{PMT or PC}}$	0.25	0.17
ND filter transmission	n/a	0.30
Stability	0.60	0.20
Temperature dependence	0.20	
Angular response$_{\text{Clear Sky(CS)}}$	1.20	0.60
Angular response$_{\text{CS,SZA}<65°}$	0.70	0.60
Angular response$_{\text{Diffuse Sky(DS)}}$	0.70	0.30
Integrated cosine error	0.30	
Measurement noise	0.20	
Measurement noise$_{\lambda=300\,\mathrm{nm,SZA}=75°}$	3.50	
Wavelength shift	0.10	
Wavelength shift$_{\lambda=300\,\mathrm{nm}}$	0.50	
Combined uncertainty	1.54	1.01
Combined uncertainty$_{\text{DS,SZA}<65°}$	1.19	0.87
Combined uncertainty$_{\lambda=300\,\mathrm{nm}}$	3.85	3.67
Expanded uncertainty$_{k=2}$	3.08	2.02
Expanded uncertainty$_{k=2,\mathrm{DS}}$	2.38	1.74
Expanded uncertainty$_{k=2,\lambda=300\,\mathrm{nm}}$	7.70	7.34

[a] Wavelength range: 310–400 nm (if not stated otherwise).

B. Stability of the 250 W Monitoring Lamp System

The spectral irradiance scale of QASUME, maintained by the 1000 W transfer standard lamps, is transferred to the lamps of the portable calibrator annually. The stability of 250 W individual lamps is checked routinely against each other by using at least three lamps during field calibrations to detect potential changes in their radiation output. The typical burning times of these lamps are between 5 and 6 h per year and the observed changes between successive calibrations of these lamps is less than 0.5%. The overall standard uncertainty due to possible lamp changes is therefore 0.14%, assuming a rectangular probability distribution of width of 0.5%.

C. Spectroradiometer Nonlinearity

Even though the data acquisition system and the photomultiplier have remained unchanged in QASUME, we have reduced the uncertainty estimation of the nonlinearity of QASUME by a factor of 2 to 0.25%, due to the fact that we operate the system at photocurrents below 1 μA, with occasional peak currents of 2 μA [2]. Furthermore, the nonlinearity of the QASUME was also measured at the TULIP setup against the reference detector, confirming the results.

For QASUMEII, which uses a photocounter, the nonlinearity correction is based on a well-proven model of dead time, as described in Section 3.C above. The dead time of the photon counter used in QASUMEII was determined to be 20 ns, with an uncertainty of 0.5 ns. By applying the nonlinearity model described in Section 3.C this results in an uncertainty in the radiation measurement of 0.17% for a nonlinearity correction of 10%, and correspondingly less for smaller nonlinearity corrections.

D. Neutral Density Filter Transmission

In order to keep the operating range of the photon counter of QASUMEII within nonlinearity corrections of less than 10%, neutral density filters are moved into the beam path at fixed wavelengths during solar UV measurements. The corresponding spectral transmittance functions of the neutral density filters were determined by measuring the corresponding spectral responsivity of QASUMEII with and without a neutral density filter inserted. The repeatability in determining the transmission was 0.5%, resulting in an uncertainty of 0.3%, as shown in Table 1.

E. Stability

It is well known that photomultipliers change their sensitivity in an unpredictable way when exposed to large doses of radiation [16]. Indeed, the responsivity of QASUME was determined several times a day using the portable lamp system while making solar UV measurements. This procedure has been repeated occasionally over the last 15 years of operation, showing that diurnal sensitivity changes of QASUME of up to 2% can be observed. Since QASUME has no continuous sensitivity monitoring implemented, the resulting diurnal variability in sensitivity results in an uncertainty contribution of 0.6% to the solar UV measurement.

In order to reduce this uncertainty component, QASUMEII uses a photodiode to continuously monitor the stability of the system. Thus, as mentioned in Sections 3.D and 4, the resulting measurement uncertainty of the photodiode at 450 nm, which is used to monitor the stability, is 0.2%.

It is worth noting that the limited dynamic range of the photocounter in QASUMEII combined with the corresponding requirement to use neutral density filters when making solar UV measurements results in a slightly larger overall uncertainty than when using an analog data acquisition system, such as the PMT in QASUME. This is compensated by the photodiode monitoring system implemented in QASUMEII, which results in an overall uncertainty of the detection system of 0.4% (combined uncertainty caused by contribution due to nonlinearity, 0.17%; ND filter transmission, 0.3%; and stability, 0.2%) with respect to the corresponding uncertainty of 0.65% for QASUME.

F. Entrance Optic

The entrance optics used by QASUME and QASUMEII were described in [2] and in Section 3.A, respectively. The measurement uncertainty of the angular response function contributes only by a small amount to the overall uncertainty estimate, especially because of the cosine weighting at large SZA where the uncertainty increases. The uncertainty of the integrated cosine error originating from the laboratory characterization is 0.3% for both spectroradiometers.

As mentioned previously, the entrance optics for both systems—QASUME and QASUMEII—are kept at a temperature of approximately 30°C. The temperature coefficient in the range 20°C to 45°C was determined to be 0.11%/K. Even though the temperature of the entrance optic is monitored, unaccounted gradients in the entrance optic introduce an uncertainty due to temperature changes of the entrance optic which we assume to be 3 K, resulting in an uncertainty of 0.2%.

One of the most significant uncertainty contributions in solar UV irradiance measurements is caused by the angular response of the entrance optic. Because of the complex radiation distribution, which is a function of solar zenith angle, wavelength and atmospheric conditions, its estimation requires the use of a complex atmospheric radiation transfer model in order to simulate the uncertainty due to this parameter. This has been discussed in [17,18]. The respective corrections assume a homogeneous diffuse radiation distribution, as well as a direct solar irradiance contribution from the unscattered solar radiation beam. The relative fractions of these two components then determine the overall correction factor for global solar irradiance measurements. In the UV part of the solar spectrum, the fraction of the diffuse and the direct irradiance is strongly modulated by the solar elevation in the sky as well as if the sun is obscured or not.

For QASUME, depending on the sky conditions, either a constant correction factor of 1.01 is applied to the measurements when only the diffuse radiation component is present (sun obscured or below the horizon) or a correction function based on solar zenith angle is used. The latter is based on clear-sky model calculations and thus represents the other extreme case. This correction function varies between 0.98 and 1.02, depending on wavelength, and for solar zenith angles between 0 and 80 deg. At larger SZA, this function converges to the diffuse correction term of 1.01. Since the model atmosphere will differ from the actual situation, and additionally the assumption of a homogeneous radiance distribution is not fulfilled [17], we follow a conservative approach and apply the full variability range of this correction function to the uncertainty budget. For QASUME, this results in an overall uncertainty of 1.2%. Assuming an overcast situation, this uncertainty is decreased to 0.7%, as is the case for wavelengths shorter than 350 nm and for SZA smaller than 65 deg.

Due to the improved angular response function of the entrance optics of QASUMEII, the corresponding uncertainties are significantly reduced: the diffuse correction term representative for overcast conditions, when there is no direct solar irradiance, is 1.005. It has an uncertainty of 0.3% resulting from the uncertainty of the angular response function determination in the laboratory. The clear-sky correction function varies between 0.99 and 1.01 as a function of SZA. The corresponding uncertainty is 0.6%.

G. Measurement Noise

The measurement uncertainty is obtained from the standard deviation of the number of measurements, N, divided by the square root of $N - 1$. Usually, seven measurements are taken within 0.7 s, which is short enough to assume constant atmospheric conditions. For wavelengths longer than 310 nm, this value is of the order of 0.2% during solar measurements, increasing sharply to 3.5% at 300 nm (see Fig. 9).

H. Wavelength Uncertainty

This uncertainty component is the uncertainty coming from a misalignment of the wavelength setting of the spectroradiometers. As discussed previously, a software algorithm adjusts the wavelength scale of each solar spectrum with respect to a high-resolution reference spectrum whose wavelength scale is traceable to SI [19]. The matSHIC algorithm was validated using solar spectra from such a Fourier transform spectrometer, yielding wavelength misalignments of up to 0.02 nm over the wavelength rage extending from 305 to 500 nm. At shorter wavelengths, matSHIC is not applicable due to the low irradiance levels and the weak Fraunhofer structure of the solar spectrum. Therefore, the wavelength shift at 305 nm is extrapolated to shorter wavelengths. Assuming a wavelength uncertainty of 0.02 nm and a rectangular probability distribution yields an uncertainty in the irradiance of 0.1% at wavelengths longer than 310 nm, increasing gradually to 0.5% at 300 nm.

I. Expanded Uncertainty

The expanded measurement uncertainty for wavelengths between 310 and 400 nm, and for solar zenith angles smaller than 75 deg, is 3.08% and 2.02% for QASUME and QASUMEII, respectively. The uncertainty is slightly lower under overcast conditions due to the decreased uncertainty associated with the angular response function. At wavelengths shorter than 310 nm, the uncertainty increases gradually to 7.70% for QASUME and 7.34% for QASUMEII due to essentially lower signal levels and the corresponding increase in measurement noise.

6. CONCLUSION

The improvements implemented during the SolarUV project have reduced the measurement uncertainties of solar spectral UV irradiance measurements from 4.8% in 2005 [2] to 2.0% in the spectral region above 310 nm, which is more than a factor of 2. The largest sources of uncertainty were the absolute spectral responsivity calibration, the angular response uncertainty, and the instrument stability, which were reduced from 3.6% to 1.1%, from 1.2% to 0.6%, and from 0.65% to 0.4% ($k = 2$), with respect to the situation prior to the project [2].

QASUMEII was successfully validated against QASUME. During a 4-month intercomparison both systems recorded over 1400 synchronized scans that could be used for the analysis. Only a few outliers of the compared solar UV spectra—ratio QASUMEII to QASUME—exceeded the expanded uncertainty of 3.7%.

To achieve this result procedures to monitor the responsivity changes of both systems were applied. For QASUME this responsivity check is carried out using a monitor system based on 250 W lamps, which is used once in a week or more often. The new hybrid detector of QASUMEII enables a continuous monitoring of the responsivity stability in addition to the lamp monitoring system. Furthermore, the cosine error of the QASUME input optics could be corrected on clear-sky days.

Both, QASUME and QASUMEII act now as reference devices for the quality assurance of solar spectral ultraviolet irradiance measurements operated by the WRC/WCCUV. With two established portable reference spectroradiometers parallel site audits and calibration campaigns can now be carried out worldwide.

Funding. EURAMET; European Union.

Acknowledgment. The research work leading to this paper was carried out within the EMRP ENV03 project SolarUV, “Traceability for surface spectral solar ultraviolet radiation.”

REFERENCES

1. M. Wild, “Global dimming and brightening: a review,” J. Geophys. Res. **114**, 2156–2202 (2009).
2. J. Gröbner, J. Schreder, S. Kazadzis, A. F. Bais, M. Blumthaler, P. Görts, R. Tax, T. Koskela, G. Seckmeyer, A. R. Webb, and D. Rembges, “Traveling reference spectroradiometer for routine quality assurance of spectral solar ultraviolet irradiance measurements,” Appl. Opt. **44**, 5321–5331 (2005).
3. G. Hülsen, “QASUME audits since 2002,” http://www.pmodwrc.ch/wcc_uv/wcc_uv.php?topic=qasume_audit.
4. J. Gröbner and P. Sperfeld, “Direct traceability of the portable QASUME irradiance scale to the primary irradiance standard of the PTB,” Metrologia **42**, 134–139 (2005).
5. M. Schuster, S. Nevas, and A. Sperling, “Validation of short-pulse-laser-based measurement setup for absolute spectral irradiance responsivity calibration,” Appl. Opt. **53**, 2815–2821 (2014).
6. M. Schuster, S. Nevas, A. Sperling, and S. Völker, “Spectral calibration of radiometric detectors using tunable laser sources,” Appl. Opt. **51**, 1950–1961 (2012).
7. L. Ylianttila and J. Schreder, “Temperature effects of PTFE diffusers,” Opt. Mater. **27**, 1811–1814 (2005).
8. G. Porrovecchio, M. Smid, J. Gröbner, M. Rajteri, C. Portesi, K. Nield, and L. Egli, “New detection systems for UV solar reference scanning spectroradiometers,” AIP Conf. Proc. **1531**, 837–839 (2013).
9. J. Mountford, G. Porrovecchio, and M. Smid, “Development of a switched integrator amplifier for high- accuracy optical measurement,” Appl. Opt. **47**, 5821–5828 (2008).
10. K. M. Nield, G. Porrovecchio, and M. Smid, Evaluation of the Linearity Performance of Silicon Trap Detectors with Switch Integrator Amplifiers at Low Optical Powers, CIE x036:2010 (2010).
11. R. D. Evans, *The Atomic Nucleus* (MacGraw-Hill, 1995).
12. L. Egli, J. Gröbner, and A. Shapiro, “PMOD/WRC annual report 2012,” http://www.pmodwrc.ch/annual_report/annualreport2012.pdf.
13. H. Slaper, H. A. J. M. Reinen, M. Blumthaler, M. Huber, and F. Kuik, “Comparing groundlevel spectrally resolved UV measurements from various instruments: a technique resolving effects of wavelength shifts and slitwidths,” Geophys. Res. Lett. **22**, 2721–2724 (1995).
14. E. Woolliams, N. Fox, M. Cox, and P. Harris, “Final report on CCPR K1-a: spectral irradiance from 250 nm to 2500 nm,” Metrologia **43**, 02003 (2006).
15. S. Nevas, J. Gröbner, M. Schuster, P. Sperfeld, L. Egli, G. Hülsen, A. Sperling, P. Meindl, S. Pendsa, and S. Pape, “Calibration of the reference spectroradiometer for the quality assurance of the terrestrial solar spectral ultraviolet radiation measurements in Europe,” in *Proceedings of NEWRAD* (2014).
16. J. Gröbner, “Progress report of the travelling reference spectroradiometer B5503: photomultiplier stability study,” Doc. EUR 20992 EN (European Commission, 2003).
17. J. Gröbner, M. Blumthaler, and W. Ambach, “Experimental investigation of spectral glabal irradiance measurement errors due to a non ideal cosine response,” Geophys. Res. Lett. **23**, 2493–2496 (1996).
18. A. Bais, S. Kazadzis, D. Balis, C. Zerefos, and M. Blumthaler, “Correcting global solar ultraviolet spectra recorded by a Brewer spectroradiometer for its angular response error,” Appl. Opt. **37**, 6339–6344 (1998).
19. P. Meindl, M. Wähmer, and C. Monte, “Usability of a Fourier transform spectroradiometer for absolute surface spectral solar UV irradiance measurements,” Opt. Express **22**, 25071–25083 (2014).